

## Three-Phase Induction Motor Parameter Estimation Using Glowworm Swarm Optimization Algorithm

V.P. Sakthivel

*Department of Electrical Engineering, Faculty of Engineering and Technology, Annamalai University, Chidambaram-608 002, India. Email: vp.sakthivel@yahoo.com*

### ABSTRACT

Imprecise parameter estimation of three phase induction motor offers inefficient control. Even if many parameter estimation approaches are available in the literature, it is yet exigent to propose an accurate parameter estimation method. In this article, glowworm swarm optimization (GSO) approach based three phase induction motor parameter estimation (TPIMPE) is introduced. The proposed TPIMPE approach exploits the nameplate data and performance characteristics of the motor. GSO algorithm is used to find the optimal equivalent circuit parameters that minimize the digression between the estimated and the manufacturer data. The viability of the proposed GSO algorithm is tested on two different sample motors and compared with the classical parameter estimation (CPE) and particle swarm optimization (PSO) based parameter estimation approaches. The simulation results divulge that the proposed TPIMPE approach competently solved the parameter estimation problems, and outperforms the CPE and PSO approaches in both solution excellence and convergence behaviors.

**Keywords** - Equivalent circuit, parameter estimation, particle swarm optimization, three-phase induction motor

### I. INTRODUCTION

The equivalent circuit parameters of three-phase induction motors are usually determined through the trials of no-load, locked-rotor and stator resistance. The parameter values determined by this classical method can reveal significant variations in the entire slip spectrum ranging from 0 to 1. Using the double-cage model, the performance features of squirrel cage induction devices can be acquired. Deep and narrow rotor bars have the same torque-speed features as double-cage rotor. Single-cage rotors should therefore be modeled as a double-cage model.

The linear parameter identification methods were used to determine the equivalent circuit parameters of a three-phase induction machine. The problem has also been solved by the sophisticated method for non-linear parameter determination [1]. A study on different techniques of detection of parameters has been discussed [2]. A simple technique for calculating induction motor parameters using IEEE standard 112 techniques has been discussed [3]. To determine the corresponding circuit parameters, no-load, blocked-rotor and overload experiments are performed. In this technique, the measuring of torque values is not utilized. The standard strategy to determining the equivalent circuit parameters of the induction motor from the accessible information was discussed [5].

These methods estimate the parameters of the machine model and then perform the sensitivity analysis with regard to the parameters of the circuit to match the information provided. A fresh parameter determination method for induction motors has been discussed in [6]. In this technique, manufacturer information such as name plate information and motor performance features were used to determine the double cage induction motor parameters. Online techniques for stator resistance and rotor resistance identification of an induction engine were suggested by Vukadinovic et al. [7].

GA [8], PSO [9], and IA [10] were used to identify induction engine parameters. Glowworm swarm optimization (GSO) suggested by Krishnanand and Ghose is a new algorithm for optimizing multimodal functions [11]. It is mimicked from the conduct that glowworms exchange data with their colleagues to search for food. GSO algorithm displays superior function to achieve the ideal solution for multimodal tasks. In this research paper, the GSO approach is used from the manufacturer information to estimate the corresponding circuit parameters of the three-phase induction motor.

The suggested GSO technique is being tested on two sample motors. The parameters acquired by the GSO technique are then used to forecast the motors' start, breakdown and full-load torques and compare

with the respective values provided by the manufacturer.

## II. PROBLEM FORMULATION

The performance characteristics required for the TPIMPE method are clustered into three load conditions of the three-phase induction motor are as follows:

- Blocked rotor condition: Power factor, stator current and torque
- Maximum torque condition: Power factor and torque
- Full load condition: Power factor, stator current, torque and efficiency

### A. Objective function

The objective of the parameter estimation problem is to discover a set of parameters that curtail the error function subjected to the constraints. The objective function  $J(X)$  is derived from the steady state equations for an induction motor. For the derivation of the steady state equations the motor equivalent circuit of Figure 1 is used. The impedance for the rotor circuits in Figure 1 is given by

$$\bar{Z}_r = \frac{R_r^1}{s} + jX_r^1 \quad (1)$$

The parallel combination of rotor impedance and magnetizing reactance is expressed by

$$\bar{Z}_f = R_f + jX_f = \frac{\bar{Z}_r \times jX_m}{\bar{Z}_r + jX_m} \quad (2)$$

The total impedance as seen from the motor terminals is defined by

$$\bar{Z}_{in} = R_{in} + jX_{in} = \bar{Z}_1 + \bar{Z}_f = R_1 + jX_1 + \frac{jX_m \times \bar{Z}_r}{jX_m + \bar{Z}_r} \quad (3)$$

$$Z_{in} = \sqrt{R_{in}^2 + X_{in}^2} \quad (4)$$

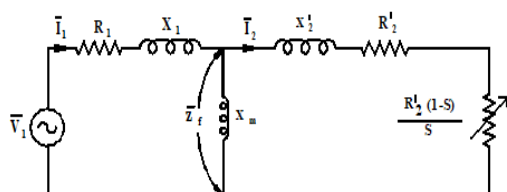


Figure 1. Equivalent circuit of an induction motor

The motor current as a function of slip follows as

$$I_1 = \frac{V_1}{Z_{in}} \quad (5)$$

The rotor circuit current as a function of slip is expressed by

$$I_2 = \frac{jX_m}{jX_m + Z_r} I_1 \quad (6)$$

From the above equations, we finally obtain the equations for current magnitude, power factor and torque:

$$I_c(S) = |I_1| \quad (7)$$

$$pf_c(S) = \cos \angle(Z_{in}) \quad (8)$$

$$T_c(S) = \frac{R_2^1}{\omega_s S} |I_2|^2 \quad (9)$$

Eqs. (7) – (9) form the basis for the objective function  $J(X)$  which is defined as a quadratic error function:

$$J(X) = W_I \sum_{i=1}^{n_I} \Delta_I^2(S_i) + W_T \sum_{i=1}^{n_T} \Delta_T^2(S_i) + W_{pf} \sum_{i=1}^{n_{pf}} \Delta_{pf}^2(S_i) \quad (10)$$

Where

$$X = [R_1, X_1, X_m, X_2^1, R_2^1] \quad (11)$$

$$\Delta_I(S_i) = \frac{I_1(S_i) - I_{m.f}(S_i)}{I_{m.f}(S_i)} \quad (12)$$

$$\Delta_T(S_i) = \frac{T(S_i) - T_{m.f}(S_i)}{T_{m.f}(S_i)} \quad (13)$$

$$\Delta_{pf}(S_i) = \frac{pf(S_i) - pf_{m.f}(S_i)}{pf_{m.f}(S_i)} \quad (14)$$

$$W_I = n_T + n_{pf} \quad (15)$$

$$W_T = n_I + n_{pf} \quad (16)$$

$$W_{pf} = n_I + n_T \quad (17)$$

### B. Constraints and boundaries

If neither constraints nor boundaries are used for the optimization, the result vector  $X$  may contain “non – physical” values, such as negative

values for parameters. Consequently, we define the following boundaries:

$$R_1, X_1, X_m, X_2^1, R_2^1 \geq 0 \quad (18)$$

Based on the nameplate data, the following three constraints are defined:

$$X_1 = X_2^1 \quad (19)$$

$$\frac{T_{\max}(X) - T_{\max \text{ m.f.}}}{T_{\max \text{ m.f.}}} \leq \pm 0.2 \quad (20)$$

$$\frac{P_{fl} - (I_{1fl}^2 R_1 + I_{2fl}^2 R_2^1 + P_{rot})}{P_{fl}} = \eta_{fl} \quad (21)$$

### III. GLOWWORM SWARM OPTIMIZATION

GSO algorithm, a fresh algorithm for swarm optimization is launched by K.N. Krishnanad and D. Ghose [23]. It mimics the motions of natural glowworms at night. The Glowworms practice in nature in a cluster, interacting and inter-attracting with each other by luciferin. If the glowworm releases lighter luciferin, more glowworms can be magnetized to move towards it. By simulating this natural phenomenon, combined with the features of natural glowworm populations, each glowworm moves to the strongest glowworm in its own field of perspective in search of the glowworm, which releases the strongest luciferin.

The GSO algorithm begins by randomly placing the glowworms in the search space so that they are well dispersed. Initially, all glowworms contain an equal amount of luciferin. Each generation consists of a luciferin-update phase, followed by a transition-based movement phase

#### A. Luciferin update phase

The luciferin update stage relies on the function value at the glowworm position and so, although all glowworms begin with the same luciferin value during the original generation, these values shift at their present roles according to the function values. During this phase, each glowworm adds a luciferin quantity proportional to the measured value of the sensed profile (fitness) at that point to its previous luciferin level. This would be the objective function value at that stage in the event of a function optimization problem. A part of the luciferin value is also subtracted to simulate the decline in luciferin over time. The luciferin update rule is defined as,

$$l_j(t+1) = \max[0, (1-\rho)l_j(t) + \gamma F_j(t+1)] \quad (22)$$

#### B. Movement phase

During this stage, each glowworm chooses to move towards a neighbor with a luciferin value more than its own using a probabilistic mechanism. This implies they are drawn to neighbors that are growing brighter. For each glowworm  $i$  the probability of shifting towards a neighbor  $j$  is represented by,

$$P_j(t) = \frac{l_j(t)}{\sum_{k \in N_i(t)} l_k(t)} \quad (23)$$

where,  $k \in N_i(t)$

$$N_i(t) = \{j: d_{ij}(t) \leq r_d^i(t); l_j(t) \geq l_i(t)\}$$

Let, the glowworm  $i$  select a glowworm  $j \in N_i(t)$  with  $p_j(t)$  is expressed in the above Eq. Then, the discrete-time model of glowworm movements can be described as

$$x_i(t+1) = x_i(t) + s \left( \frac{x_j(t) - x_i(t)}{\|x_j(t) - x_i(t)\|} \right) \quad (24)$$

Where,  $S = \begin{cases} \delta & \text{if } d_{ij}(t) \geq \delta \\ d_{ij}(t) & \text{otherwise} \end{cases}$

#### C. Local-decision range update rule

When the glowworms rely on only local data to determine their motions, the number of peaks recorded is anticipated to be a powerful function of the radial sensor range. For example, if each agent's sensor ranges cover the entire workspace, all agents move to the optimum global point, and the local optima is ignored. Since we regarded that prior data about the objective function is not accessible, in order to detect different peaks, a varying parameter must be made of the sensor range. To this end, we combine each agent  $i$  with a local decision domain whose radial range  $r_d^i$  is dynamic in nature  $0 \leq r_d^i \leq r_s^i$ . The appropriate function is chosen to adapt the local-decision domain variety of each glowworm and is expressed by,

$$r_d^i(t+1) = \min[rs, \max[0, r_d^i(t) + \beta(n_t - |N_i(t)|)]] \quad (25)$$

### IV. SOLUTION METHODOLOGY

To demonstrate the adequacy of the GSO, it is applied to solve the TPIMPE problem. The issue solving algorithm based on the suggested technique is as follows:

- Step 1:** Read the specifications and the manufacturer data of the motor.
- Step 2:** Read GSO algorithm parameters.
- Step 3:** Initialize initial luciferin value  $l_0$  and local decision range  $r_0$ .
- Step 4:** Initialize the glowworm within the limits of each variable.
- Step 5:** Find the objective value using Eq. (10) and the luciferin value of all glowworms using Eq. (22).
- Step 6:** Find the neighborhood glowworms having brighter glow and are in the local decision range.
- Step 7:** Find the probability of glowworm moving towards a neighbor using Eq. (23).
- Step 8:** Update the glowworm movement using Eq. (24) and check the limits.
- Step 9:** Update the local decision range of all glowworms using Eq. (25).
- Step 10:** Repeat the above steps 5 to 9, until maximum iterations are attained.
- Step 11:** Display the optimal equivalent circuit parameters and their corresponding performance characteristics of the motor.

slip, power factor-slip and current slip characteristics of the test motors respectively. In order to verify the performance of the proposed GSO based TPIMPE, the comparisons of CPE and PSO approaches are provided.

The parameters used in GSO parameters are as follows:

- Luciferin decay constant = 0.97,
- Luciferin enhancement constant = 0.97,
- Constant parameter = 0.0005;
- Neighborhood threshold (nt) = 4;
- Radial range of Luciferin sensor (rs) = 0.005; and
- Local decision domain range (rd) = 0.0005.

## V. EXPERIMENTAL RESULTS

The proposed GSO based TPIMPE problem is tested on two sample motors. Tables 1 presents the information's of the nameplate data, and the torque-

**Table 1.** Name plate data of the test machines

Specifications	Motor 1	Motor 2
Capacity	5 HP	40HP
Voltage	400V	400V
Current	8A	45A
Frequency	50 Hz	50Hz
No. of poles	4	4
Full load slip	0.07	0.09
Full load torque	25 Nm	190Nm
Full load efficiency	88%	90%

**Table 2.** Comparison of CPE, PSO and GSO with manufacturer data for motor 1

Characteristic	Manufacturer data	CPE		PSO		GSO	
		Estimated data	Error (%)	Estimated data	Error (%)	Estimated data	Error (%)
Starting torque (Nm)	15	14.25	5	16.0115	-6.74	16.02	-6.7
Starting current (A)	22	21.722	1.27	22.29	-1.33	23.27	-5.53
Maximum torque (Nm)	42	36.46	13.18	41.84	0.38	41.63	4.9
Full load torque (Nm)	25	27.415	-9.66	27.635	-10.54	27.35	-9.76
Full load current (A)	8	7.82	2.24	7.4	7.42	7.53	6.32
Full load power factor	0.8	0.88	-10.09	0.829	-3.63	0.76	1.84
Full load efficiency (%)	88	83.22	5.44	90.57	-2.93	90.45	-2.86

**Table 3.** Comparison of CPE, PSO and GSO with manufacturer data for motor 2

Characteristic	Manufacturer data	CPE		PSO		GSO	
		Estimated data	Error (%)	Estimated data	Error (%)	Estimated data	Error (%)
Starting torque (Nm)	260	265.238	-2.01	255.68	1.66	255.72	1.68
Starting current (A)	180	190.56	-5.8	183.89	-2.16	184.52	-2.66
Maximum torque (Nm)	370	394.71	-6.7	380.48	-2.83	377.93	-2.56
Full load torque (Nm)	190	178.17	6.22	172.6	9.16	170.58	10.74
Full load current (A)	45	43.616	3.07	42.32	5.96	41.790	7.32
Full load power factor	0.8	0.829	-3.6	0.833	-4.17	0.84	-2.46
Full load efficiency (%)	90	90.646	-0.72	90.492	-0.55	90.63	0.58

**Table 4 .** Comparison of results for 20 runs of PSO and GSO approaches

Values	Motor 1		Motor 2	
	PSO	GSO	PSO	GSO
Minimum	0.01863	0.0207	0.00247	0.0023
Maximum	0.0285	0.0215	0.0036	0.0026
Deviation (%)	53	7.65	45.75	7.5

The error (e) is computed as follows:

$$e (\%) = \frac{X_{m.f.} - X_c}{X_{m.f.}} \times 100 \quad (26)$$

The results of GSO based TPIMPE approach are compared with CPM and PSO techniques in Tables 2 and 3 for test motors 1 and 2 respectively. As can be seen in Tables, the performance characteristics of the model using the equivalent circuit parameters of GSO algorithm show remarkable agreement with the manufacturer data in the entire slip range. Also the error is computed for each performance characteristic of the motor.

Due to the randomness in the stochastic approaches, these approaches are run by 20 times with the test motors. The statistical results obtained by GSO and PSO approaches are tabulated in Table 4. These results show that the motor parameters estimated by the GSO algorithm lead to objective value less than that found by other approaches, which confirms that the GSO is suitable for estimating the global optimum solution.

Figure 2 illustrates the convergence features and demonstrates the effect of random initialization generated by the suggested GSO technique. These provide quick convergence and robustness with regard to the original group of the GSO algorithm.

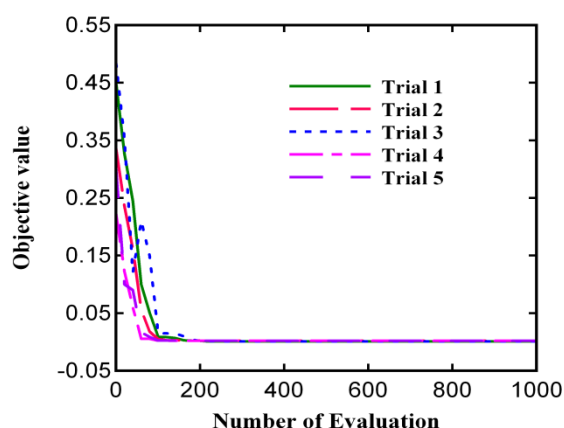


**Figure 2.** Convergence characteristics of the GSO for different initial group

## VI. CONCLUSION

In this paper, a swarm intelligence approach, GSO is presented for solving the parameter estimation of three-phase induction motor. The GSO algorithm is used to minimize the digression between the estimated and the manufacturer data. The TPIMPE approach is applied on two sample motors and the results are compared with the classical and PSO based parameter estimation approaches. The GSO based TPIMPE approach provides better solution excellence and convergence behavior than the other approaches. This TPIMPE approach can be implemented for all capacities of the motor. From this comparative study, it can be concluded that the GSO approach can be used for multi-dimensional engineering optimization systems such as parameter estimation, electrical machine design and power system problems.

## NOMENCLATURE

$V_1$	Stator voltage per phase (V)
$I_1, I_2$	Stator current and rotor current per phase respectively (A)
$R_1$	Stator resistance per phase ( $\Omega$ )
$X_1$	Stator leakage reactance per phase ( $\Omega$ )
$R_2^1$	Rotor resistance referred to stator side ( $\Omega$ )
$X_2^1$	Rotor reactance referred to stator side ( $\Omega$ )
pf	Power factor
$T_{max}$	Pullout or maximum torque (Nm)
$\omega_s$	Motor's angular velocity (rad /sec)
$\eta_{fl}$	Full load efficiency (%)
$S_i$	Discrete slip values
$S_{fl}$	Full load slip
c and m.f.	Calculated and manufacturer value respectively.
$n_i, n_{pf}$ , and $n_T$	Total number of data points available for current, power factor and torque respectively
$W_i, W_{pf}$ and $W_T$	Weighting factor for current, power factor and torque respectively
$P_{fl}$	Rated power (W)
$P_{rot}$	Rotational losses (W)
$X_{m.f.}$ and $X_c$	Manufacturer and calculated data of performance characteristic X

## REFERENCES

- [1] K. Wang, J. Chiasson, M. Bodson, L.M. Tolbert, 2005. A Nonlinear Least Squares Approach for Identification of The Induction Motor Parameters, IEEE Transactions on Automatic Control, vol. 50, n. 10, 2005, pp.

- 1622-1628.
- [2] H.A. Toliyat, E. Levi, M. Raina, A Review of RFO Induction Motor Parameter Estimation Techniques, *IEEE Transactions on Energy Conversion*. Vol. 18, n. 3, 2003, pp. 271-283.
- [3] J. Pedra, L. Sainz, Parameter Estimation of Squirrel-Cage Induction Motors without Torque Measurements, *IEE Proceedings - Electric Power Applications*, vol. 153, n. 2, 2006, pp. 263-269.
- [4] J. Pedra, F. Corcoles, Estimation of Induction Motor Double-Cage Model Parameters from Manufacturer Data, *IEEE Transactions on Energy Conversion*, vol. 19, n. 2, 2004, pp. 310-317.
- [5] D. Lindenmeyer, H.W. Dommel, A. Moshref, P. Kundur, An Induction Motor Parameter Estimation Method, *Electrical Power and Energy Systems*, vol. 23, 2001, pp. 251-262.
- [6] D. Vukadinovic, M. Basic, L. Kulisic, An IRFO System with Stator and Rotor Resistance Identification for the Induction Motor, *International Review of Electrical Engineering*, vol. 3, n. 4, 2008, pp. 709-720.
- [7] Tooraj Abbasian Nadjafabadi, Farzad Rajaei Salmasi, A Flux Observer with Online Estimation of Core Loss and Rotor Resistances for Induction Motors, *International Review of Electrical Engineering*, vol. 4, n. 5, 2009, pp. 816-824.
- [8] E. Rahimpour, V. Rashtchi, M. Pesaran, Parameter Identification of Deep-Bar Induction Motors Using Genetic Algorithm, *Electrical Engineering*. vol. 89, 2007, pp. 547-552.
- [9] V.P. Sakthivel, R. Bhuvaneswari, S. Subramanian, Multi-Objective Parameter Estimation of Induction Motor Using Particle Swarm Optimization, *Engineering Applications of Artificial Intelligence*, vol. 23, n. 3, 2010, pp. 302-312.
- [10] V.P. Sakthivel, R. Bhuvaneswari, S. Subramanian, Artificial Immune System for Parameter Estimation of Induction Motor, *Expert Systems with Applications An International Journal*, vol. 37, n. 8, 2010, pp. 6109-6115.
- [11] Krishnand K N, Ghose D. Glowworm swarm optimization for simultaneous capture of multiple local optima of multimodal functions. *Swarm Intelligence* 2009; 3 (2):87-124.